1991

Foundations of linear control via a new geometric paradigm

Thomas R. Kurfess
Carnegie Mellon University

Mark L. Nagurka

Carnegie Mellon University.Engineering Design Research Center.

Foundations of Linear Control Via a New Geometric Paradigm

T. Kurfess, M. Nagurka

EDRC 24-71-91

Foundations of Linear Control Via a New Geometric Paradigm

by

Thomas R. Kurfess **Mark L. Nagurka**

September 1991

Abstract - **In this report, we reexamine the foundations of classical control theory with reference to eigenvalue geometry via a new set of graphical controls tools, gain plots. These plots depict eigenvalue trajectory as an explicit function of gain. Various classical control concepts are generalized in nine theorems and demonstrated in three simple, yet pedagogical, examples.**

The authors are with the Department of Mechanical Engineering, Carnegie Mellon University, Pittsburgh, PA.

I. Introduction

There have been many important developments in classical control theory of linear time-invariant (LTI) systems as a result of geometric perspectives (Nyquist, Bode, Evans) [1-3]. These graphical methods remain key control analysis and design tools even in the post-computer age. In fact, the advent of the computer has extended these methods considerably. For example, multivariable root locus plots can be generated as readily as single-input, single-output (SISO) root locus plots. The power and availability of software tools has prompted us to consider a new geometric perspective of the Evans root locus. The resulting plots, called gain plots (GPs), show the explicit variation of eigenvalue magnitudes and angles with respect to a scalar system parameter, such as forward gain [4], The eigenvalue magnitude *vs.* gain is portrayed in a magnitude gain plot (MGP) using a log-log scale and the eigenvalue angle *vs.* gain is displayed in an angle gain plot (AGP) using a semi-log scale (with the logarithms being base 10). Although we select gain as the variable of interest, it should be noted that any parameter may be used in the geometric analysis.

In this report we employ the standard state-space representation of an LTI system:

$$\dot{x}(t) = Ax(t) + Bu(t) \tag{1}$$

$$y(t) = Cx(t) + Du(t) \tag{2}$$

where xe $9?_n$ is the state, u€ $9i_m$ is the plant command or control input, ye $9?_m$ is the plant output, and {A, B, C, D}e 9f with appropriate dimensions. The input-output dynamics are governed by a square transfer function matrix, G(s),

$$G(s) = C[sI - A]^{1}B + D \tag{3}$$

The system is embedded in a unity feedback closed-loop configuration with forward static compensator, kl, implying that each input channel is scaled by the same constant gain k. (Note that the plant transfer function matrix and any dynamic compensation may be combined in the transfer function matrix G(s).) The control law is given by

$$u(t),= kle(t) \tag{4}$$

where

$$e(t) = r(t)-y(t) \tag{5}$$

is the error and r(t) € 9f$_m$ is the reference (command) signal that y(t) must track. The **closed-loop transfer function** matrix is

$$Gc_L(s) = [I-HkG(s)]^{-1}kG(s) \quad (6)$$

To develop the root locus plot, the migration of the eigenvalues of GCL(S) in the complex plane is portrayed for 0 £ k < °°. The eigenvalues of the closed-loop system, s = X_x (i=l,2,...,n), are the roots of <t>cL(s)> the closed-loop characteristic polynomial,

$$\phi_{CL}(s) = <|>oL(s)\det[I + kG(s)] \quad (7)$$

where <1>OL(S) is the open-loop characteristic polynomial,

$$\phi_{OL}(s) = \det[sI - A] \quad (8)$$

The roots of (8) are the open-loop poles; they are also the eigenvalues of A. By equating the determinant in (7) to zero, the multiple-input, multiple-output (MIMO) generalization of the SISO characteristic equation (1 + kg(s) = 0) is obtained. The presence of the determinant is the major challenge in generalizing the SISO root locus sketching rules to MIMO systems and complicates the root locus plot. For example, the root locus branches "move" between several copies (Riemann sheets) in the s-plane that are connected at singularity points known as branch points [5,6].

Although it is not normally possible to sketch MIMO root loci by inspection, the closed-loop system eigenvalues may be computed numerically from

$$\lambda_i = eig\left[A - B(I + kD)^{-1}kC\right] , \quad i = 1, 2, \ldots, n \quad (9)$$

where eig[Q] represents the eigenvalues of matrix Q. In the examples, the loci of the eigenvalues are calculated from (9) as k is monotonically increased from zero.

II. Geometric Paradigms of Fundamental Control Concepts

This **section** presents a series of theorems that encapsulate fundamental concepts of classical control theory. Some of these concepts are discussed openly in the literature, while others do not seem to be mentioned. These theorems demonstrate the insight into control theory fundamentals provided by the GPs.

We introduce two assumptions:

Assumption 1: The systems analyzed are lumped parameter LTI systems.

Assumption 2: The forward scalar gain, k, is real and positive, *i.e.*, k *e* 9f, k > 0.

Open—Loop Eigenvalue Representation

Theorem 1:

$$\lim_{k \to 0} Ri(k) = |eig(A)|, \quad i = 1, \ldots, n \tag{10}$$

$$\lim_{k \to 0} 0_I(k) = Z(eig(A)), \quad i = 1 \ldots n \tag{11}$$

where R* and 0j, are the MGP and AGP ordinate values, respectively.

Proof: It follows from (7) that

$$\lim_{k \to o} 0CL(S) = \lim_{k \to 0} 0oL(s)\det[I + kG(s)] = 0OL(S) \tag{12}$$

which is the open-loop case.

Root Locus 180° Criterion

Theorem 2: Curve segments on the AGP must either lie on a multiple of 180" or must occur in a set of two segments that are symmetric about .i multiple of 180°.

Proof: Since (A, B, C, D} *e* 9f, then (9) represents the standard eigenvalue equation

$$\lambda I - (A - B(I + kD)^{-1}kC)\, I = 0 \tag{13}$$

generating a polynomial in *X* with real coefficients. Therefore, any complex eigenvalue must occur in a complex pair.

High Gain Behavior of Infinite Magnitude Eigenvalues

As k increases from 0 to <», the closed-loop eigenvalues trace out "root loci" in the complex plane. At zero gain, the eigenvalues of the closed-loop system are the open-loop poles. At infinite gain some of these eigenvalues approach finite transmission zeros, defined to be those values of $z\backslash$ that satisfy the generalized eigenvalue problem

$$\begin{bmatrix} z & \\ & C \end{bmatrix} - \begin{bmatrix} & \\ & D \end{bmatrix} \quad \text{HrKsj.'--'."-} \tag{14}$$

where [**x(0) v**]^r is **the** right generalized eigenvector corresponding to the generalized **eigenvalue,** /•#:, transmission zero, with x(0) representing the initial state and **v** being a **vector representing input** direction in the multi-input case. In the absence of pole/zero **cancellation, the finite** transmission zeros are the roots of the determinant of G(s). **Algorithms have been developed** for efficient and accurate computation of transmission **zeros** [7-9]. Those eigenvalues that do not have matching zeros in the finite part of the s-**plane are considered** to have matching zeros at infinity; these are the *infinite* eigenvalues. An interesting perspective of the high gain SISO'root locus behavior is presented in [10].

Theorem 3: For SISO systems with n poles and m transmission zeros

$$\lim_{k\to\infty} \theta \qquad n \cdot \tag{15}$$

where there are n-m 0 values corresponding to the n-m infinite eigenvalues. This is the Butterworth configuration [11].

Theorem 4: For SISO systems with n poles and m transmission zeros

$$\lim_{k\to\infty} R_i = k^{1/(n-m)}, \quad i = m+1,\ldots, n \tag{16}$$

where there are n-m magnitude values corresponding to n-m infinite eigenvalues.

Proof: An LTI SISO system may be characterized by the transfer function

$$g(s) = \frac{n(s)}{d(s)} = \frac{\sum_{i=0}^{m} b_i s^i}{\prod_{j=0}^{n} a_j s^j} \tag{17}$$

where n(s) is the transfer function numerator of order m in s with coefficients, b,· (i=0, 1, ..., m), **and** d(s) **is the transfer** function denominator of order n in s with coefficients, a_n **0=0, 1,..., n) with a_n=l. 4>CL(S) is**

$$\text{0CL(S)} = \mathbf{d(s) + kn(s)} = \sum_{j=0}^{n} \mathbf{a_j s^j} + \mathbf{k} \sum_{i=\diamond}^{m} \mathbf{M} \tag{18}$$

which can be written as

$$k = -\frac{d(s)}{n(s)} \approx -\frac{\sum_{i=0}^{n} a_j s^j}{A} \qquad (19)$$

From (19), as k->©o, the ratio of n(s) to d(s) must also tend towards infinity at the same **rate.** As **k—><»**, there are two possibilities for the magnitude ratio of d(s) to n(s), *i.e.*,

$$n(s) \to 0 \qquad (20)$$

and/or

$$d(s) \to \infty \qquad (21)$$

In **the** literature, it is shown that both of these criteria are satisfied as k—»oo. For large gain, the highest order s term for both d(s) and n(s) dominates, since lsl-**>. Thus, in the limit as k—><», (19) may be approximated by

$$k \approx -\frac{b}{t} \qquad (22)$$

From (22), the asymptotic behavior of the eigenvalues may be realized as

$$\lambda = \ldots \qquad (23)$$

By taking the magnitude and angle of X. in (23), the proof for *Theorems 3* and *4* is completed.

Eigenvalue Approach Rates to Transmission Zeros

Theorem 5: For SISO systems with m transmission zeros

$$\lim_{k \to \infty} |z_i - \lambda| = k^{1/w_i}, \quad i = 1, \ldots, m \qquad (24)$$

where wj is the transmission zero multiplicity at z\ in the complex plane.

Before the proof is presented, we make the following assumption.

Assumption 3: There are no open-loop pole/zero cancelations. That is

$$p_j \neq z_i \quad \forall j, i \qquad (25)$$

where pj and z\ are the poles and zeros of the system, respectively.

Proof: **For** (20) to hold,

$$\lim_{k \to \infty} \lambda_i = z_i , \quad i = 1, \ldots, m \tag{26}$$

since **the** zfs **are the** roots of n(s).

Rewriting (19) as the ratio of products

$$k = -\frac{\prod_{j=1}^{n} (s + p_j)}{\prod_{i=1}^{m} (s + z_i)} \tag{27}$$

and evaluating it at

$$s = \lambda_i \rightarrow z_i \tag{28}$$

we recognize that k—»©0, as (28) and consequently (20) are realized. Furthermore, since *z{* are defined as the *finite* transmission zeros, s - pj must be finite, and s - *zy* * 0 (due to *Assumption 3)* if *z*\ * ZJ' where i' * i. In general, if there are w multiple poles at *z*

$$\lim_{k \to \infty} \left[\frac{\prod_{j=1}^{n} (s + p_j)}{\prod_{i=1}^{m} (s + z_i)} \right]_{s = \lambda_i} = \lim_{\lambda_i \to z_i} \left[\frac{\prod_{j=1}^{n} (s + p_j)}{\prod_{i=1}^{m} (s + z_i)} \right]_{s = \lambda_i} , \quad i = 1, \ldots, m \tag{29}$$

and

$$X\backslash + p_j = \alpha_j, \quad i = 1, \ldots, m ; \quad j = 1, \ldots n \tag{30}$$

where ctj is a constant, and

$$\lambda_i + z_{i'} = \beta_{i'} , \quad z_{i'} \neq z_i ; \quad i = 1, \ldots, m \tag{31}$$

where Pr is a constant.

Thus

$$\lim_{\lambda_i \to z_i} \left[\frac{\prod_{j=1}^{n} (s + p_j)}{\prod_{i=1}^{m} (s + z_i)} \right]_{s = \lambda_i} = \lim_{\lambda_i \to z_i} \left[\frac{A_i}{B_i (s + z_i)^w} \right]_{s = \lambda_i} , \quad i = 1, \ldots, m \tag{32}$$

where

$$A_i = \sum_{j=1}^{n} a_j, \quad i = 1, \ldots, n \tag{33}$$

and

$$B_i = \sum_{\substack{i'=1 \\ i' \neq i \\ z_{i'} \neq z_i}}^{m} P_{i'} \tag{34}$$

completing the proof.

Stability

Theorem 6: If the principal angle of the closed-loop system eigenvalues is

$$0° \leq \theta < 360° \tag{35}$$

then the system is stable if

$$90° < \theta < 270° \tag{36}$$

Outside this range, the system is unstable.

Proof: Since the AGP depicts the angle of the system eigenvalues, eigenvalues having angles in the range given by (36) are in the right hand plane yielding unstable differential equations. This is the classical root locus stability criterion.

Gain Margin

Theorem 7: For a given gain, k, the gain margin, GM, of the closed-loop system may be computed from the AGP as

$$GM = 20 \log \left| \frac{N}{K} \right| (db) \tag{37}$$

where k_s is the gain corresponding to marginal stability.

Proof: In the frequency domain, GM is defined as

$$GM = 20 \log |k_s (g(j\omega_a))| - 20 \log |k (g(j\omega_a))| \, (db) = 20 \log \left| \frac{k_s}{k} \right| (db) \tag{38}$$

where

$$\angle g(j\omega_a) = -180^\circ \tag{39}$$

(38) may **be amplified** as

$$\mathbf{GM} = 20 \log\left(\left|\frac{k_s}{k}\right| \left|\frac{g(jCOa)}{g(j\omega_a)}\right|\right)(db) = 20iog|^|(db) \tag{40}$$

This ratio is the factor by which k may be increased before instability occurs. Both the numerator and denominator of (40) may be determined by inspection from the AGP.

Root Sensitivity Function

In classical control theory the root sensitivity, S_p, is defined as the relative change in the system roots or eigenvalues, $X\backslash$ (i = 1,..., n), with respect to a system parameter, p. Most often, the parameter analyzed is the forward proportional controller gain, k. **The root** sensitivity with respect to gain is given by

$$\mathbf{S\,t} = \frac{d\lambda(k)/\lambda(k)}{dk/k} = \wedge \mathbf{i\ r}\ \ddot{\wedge} \qquad <^{4}\!\!\text{»}\ \ \mathbf{!}$$

Since the eigenvalues may occur as complex conjugate pairs, *Sk* may be complex.

Assumption 4: There are no eigenvalues at the origin of the s-plane, *i.e.*,

$$X\backslash * 0\ ,\ \text{Vi} = 1,\ ...,\ n \tag{42}$$

However, the theorems are valid for eigenvalues arbitrarily close to the origin singularity.

Based on these assumptions, we draw the following theorems.

Theorem 8: The real component of the sensitivity function is given by

$$\text{Re}\ \{\text{Sit}\} = \text{Af}_m \tag{43}$$

where M_m is **the** slope of the MGP.

Theorem 9: The imaginary component of the sensitivity function is given by

$$\text{Im}\ \{S_k\} = \frac{1}{\log e} Ma \tag{44}$$

where M_a is the slope of the AGP.

Proof: Equation (41) may be rewritten [12,13j in terms of the derivatives of natural logarithms as

$$S_k = \frac{d\ln(X(k))}{d\ln k}\bigg|_T \tag{45}$$

The natural logarithm of **the** complex value, *X*, may be written as the sum of the logarithm **of the magnitude of *X* and the angle of *X* multiplied by j = I^T. Thus, (45) becomes**

$$S_* = \frac{d\ln|X(k)|}{d\ln(k)} + j\frac{d\angle X(k)}{d\ln(k)} = \frac{d\log|X(k)|}{d\log(k)} + j\frac{1}{\log e}\frac{d\angle X(k)}{d\log(k)} \tag{46}$$

The complex root sensitivity function is now expressed **with distinct real and imaginary components employing** the polar form of the eigenvalues. Since **k** is **real and positive, d ln(k) and d** log(k) are purely real obviating the need to decompose **those terms into polar form. (In general,** most parameters studied are real and this **proof** is **sufficient. If, however, the** parameter analyzed is complex, it is a straightforward task **to extend the above** analysis.) Equation (46) may be rewritten as

$$S_k = M_m + \frac{1}{\log e} M_a \tag{47}$$

The proof is completed by taking the real and imaginary components of (47), yielding (43) and (44). It is interesting to note that the Cartesian **representation of 5* is related to the polar** representation of *X*\.

IV. Examples

Example 1

To demonstrate the theorems presented above, we examine a second order system with **a** PD controller.

(48)

This system has open-loop poles at s = - 1 , s = -2 and a finite transmission **zero at** s = - 3 . **Hence, n = 2 and m** =1 in the notation employed earlier. The root locus of **(48)** is **presented in Figure 1. It** shows a break-out point at s ~ -1.6, a break-in **point at** s * **-4.4, Butterworth** asymptotes along -180°, and reveals that the closed-loop system is stable given Re(Xi) < 0, V i,k.

An alternate representation of Figure 1 is the MGP of Figure 2a and the **AGP** of Figure 2b. Here, the explicit influence of gain on the eigenvalue trajectories is represented. As k -» 0 the MGP and AGP reveal the influence on the magnitudes and angles,

respectively, of the open-loop eigenvalues demonstrating *Theorem 1.* The curve segments **in the AGP are either on the** 180# line or symmetric about it, in agreement with *Theorem 2.* **Also, the break-out and** break-in points are evident at k * 0.17 and k » 5.83, respectively. **As** k -» °° **the AGP shows the** Butterworth configuration for a single infinite eigenvalue **proceeding along a trajectory** of 180* in accordance with *Theorem 3. Theorem 4* is **demonstrated** by **the** corresponding high gain MGP slope of unity for the infinite **eigenvalue.**

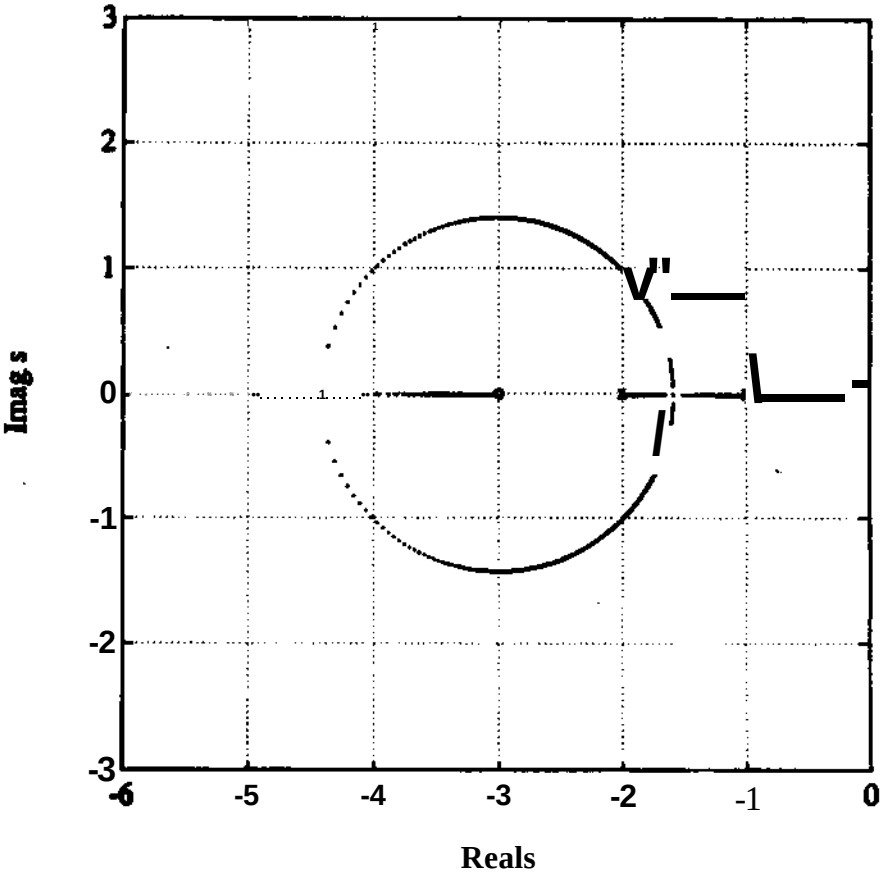

Figure 1. Root Locus Plot for Example 1.

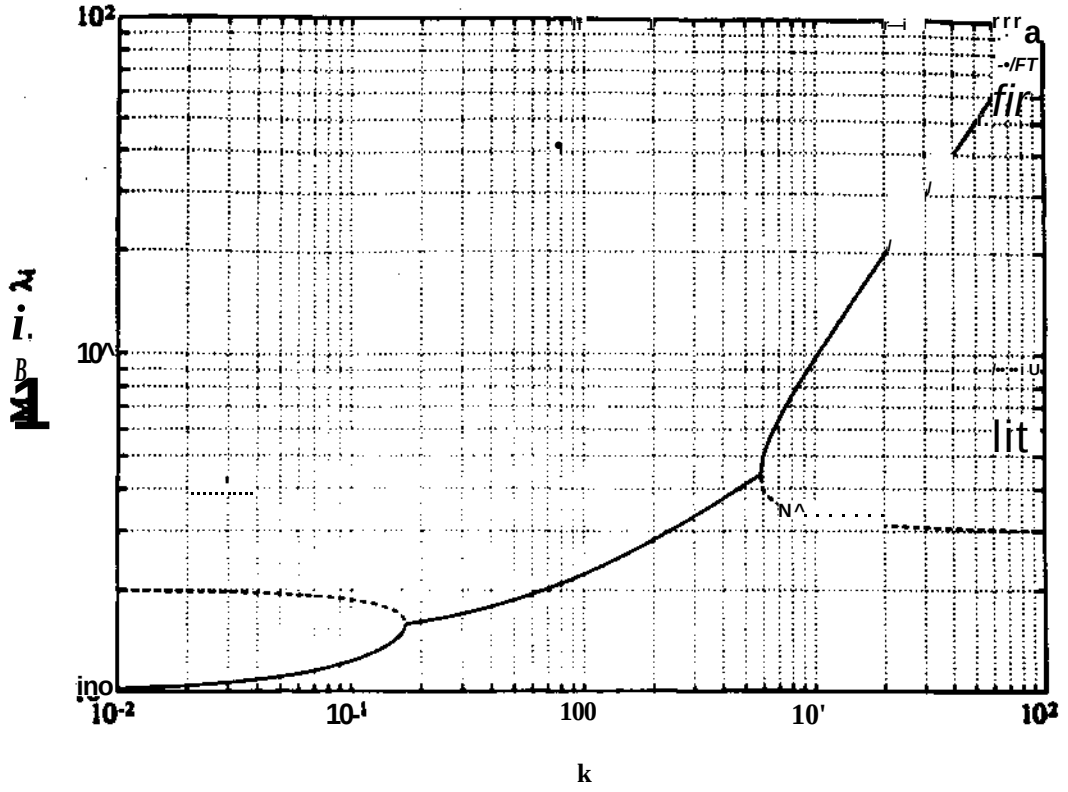

Figure 2a. Magnitude Gain Plot for Example 1

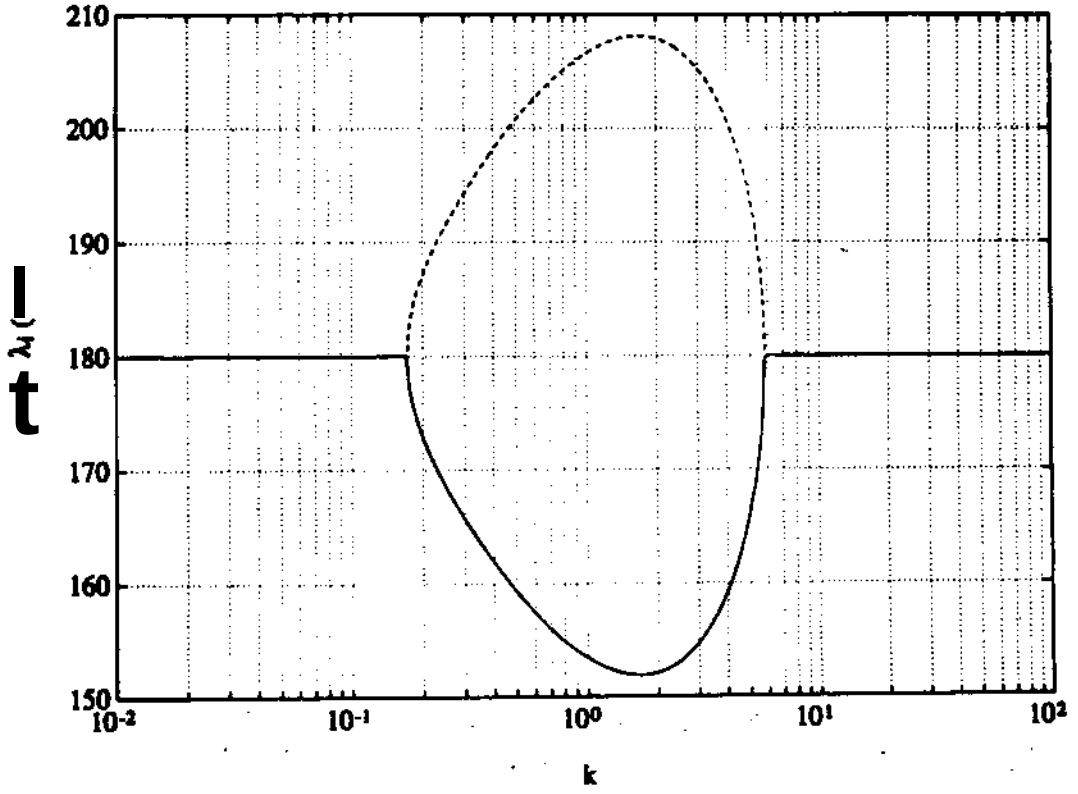

Figure 2b. Angle Gain Plot for Example 1

To observe the approach rate to the finite transmission zero, we have constructed **a modified MGP^fcich shows the** distance of the finite eigenvalue to the finite zero at s = -L **The resulting figure, Figure** 3, shows that as k -» <» the distance is inversely proportional **to k confirming *Theorem*** *5* for w = 1. Figure 3 also shows that between the break points **there is a constant distance** between the eigenvalue and the transmission zero, **demonstrating that the** eigenvalue trajectory about the transmission zero is circular in the **complex plane.**

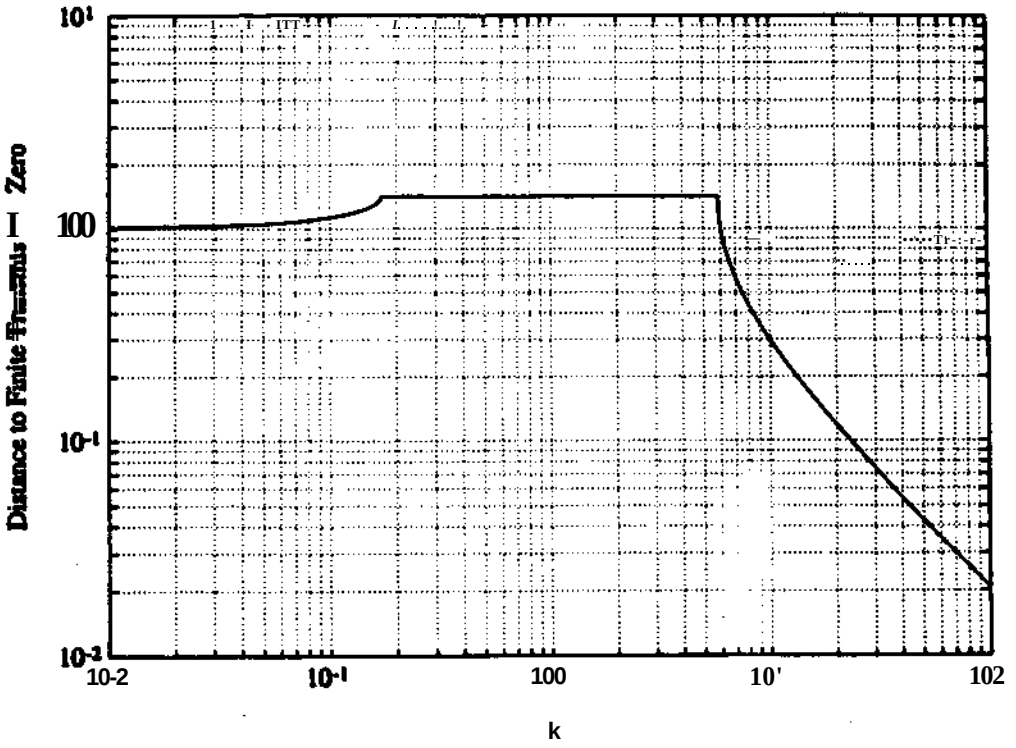

Figure 3. Distance to Single Finite Transmission Zero for Example 1.

Since 9j is always in the range prescribed by (36), the closed-loop system is stable **for all gains, and hence has an** infinite gain margin. A more interesting demonstration of *Theorems 6* **ami** 7 follows in Example 2.

***Theorems 8* and 9 are** demonstrated by the sensitivity plots of Figures 4a and 4b, **respectively.** (These figures were generated from (45) by plotting the real and imaginary components of S*.) They clearly highlight the infinite sensitivities at the break points. Furthermore, they show the sensitivity function is real for *X\ e* 9f. The crossover point at k « 2 in Figure 4b corresponds to the extremum of Im{Xi}. As k —> 00 the finite eigenvalue becomes completely desensitized whereas the infinite eigenvalue has a sensitivity of unity, again confirming *Theorems 8* and 9.

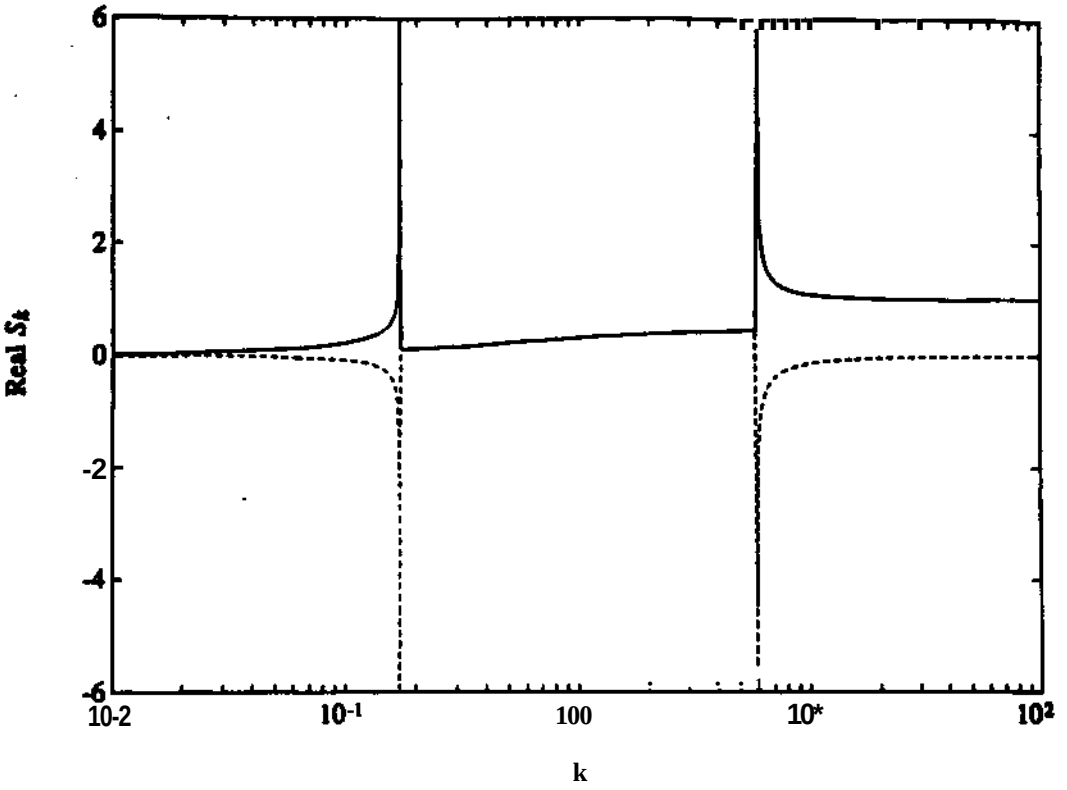

Figure 4a. Real Component of Sensitivity for Example 1.

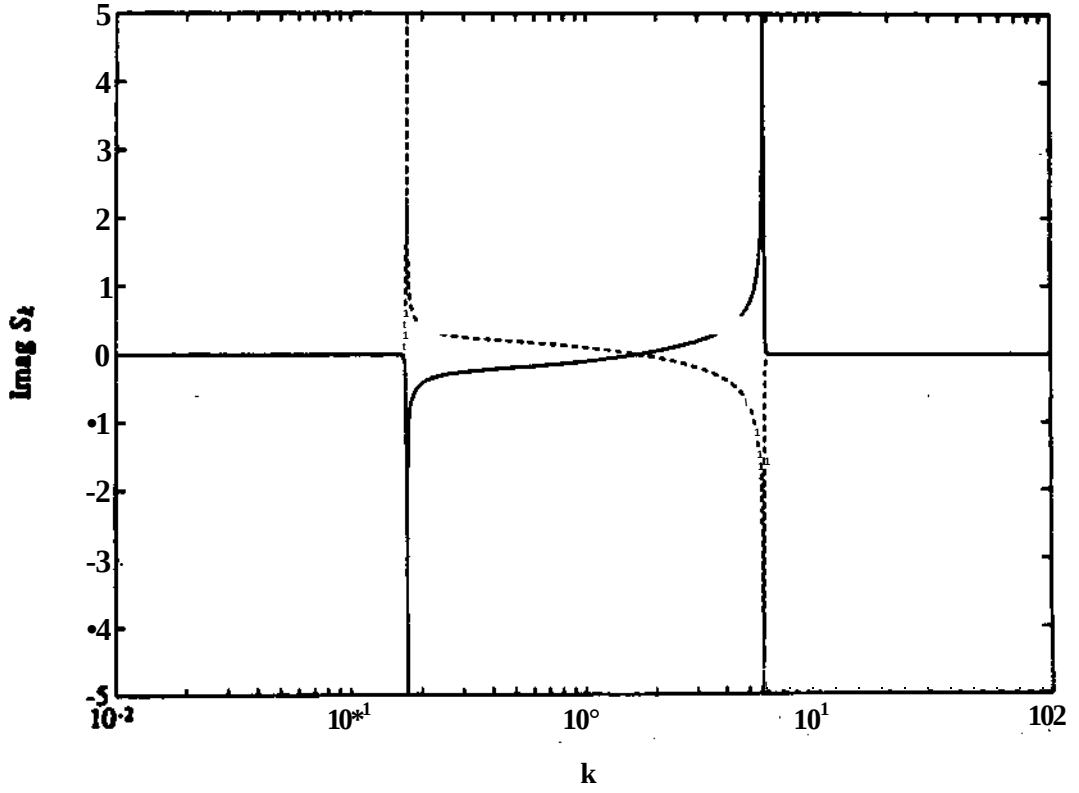

Figure 4b. Imaginary Component of Sensitivity for Example 1.

Example 2

This example **[14]** considers a third order system (with a transmission zero) employing integral control.

$$g_2(s) = \frac{s+1}{s(s-1)(s+10)^2} \tag{49}$$

This system is open-loop unstable. The root locus plot of Figure 5 shows that there is a regime for which the closed-loop system is stable. The corresponding gain plots are shown in Figures 6a,b. It is possible using *Theorem 6* to determine the stable range as $132 < k < 1230$. From *Theorem 7* the gain margin can be computed at any design value of k. For example, at $k = 300$, the lower gain margin is $20\log(132/300) \approx -7.1$ dB and the upper gain margin is $20\log(1230/300) \approx 12.3$ dB.

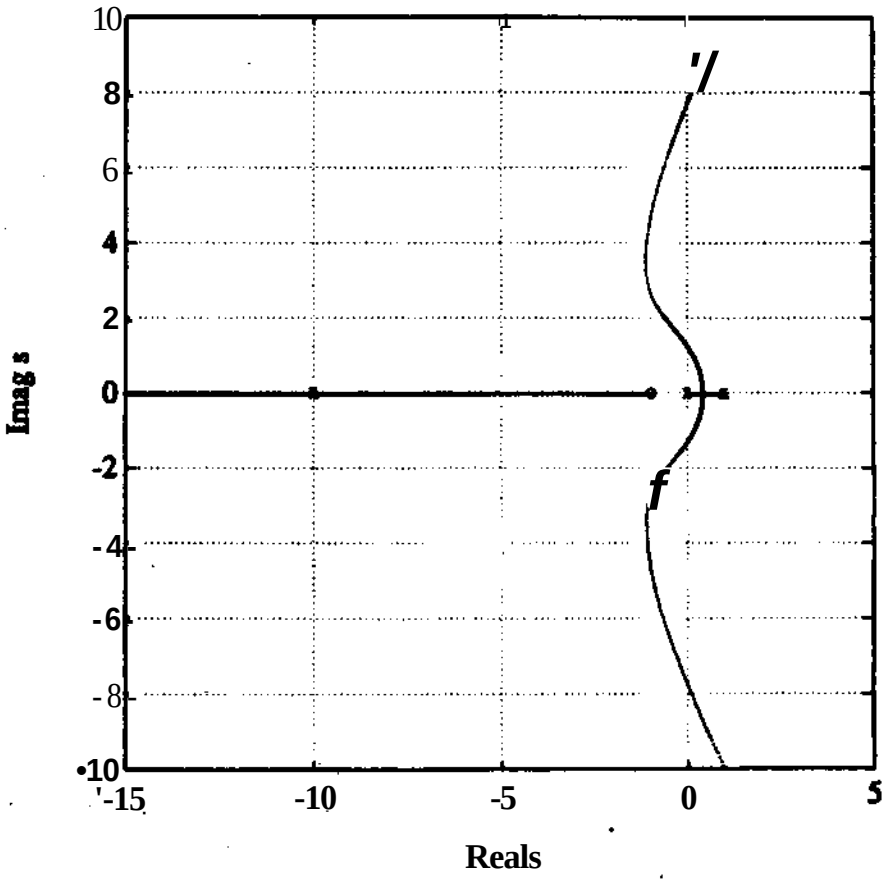

Figure 5. Root Locus Plot for Example 2.

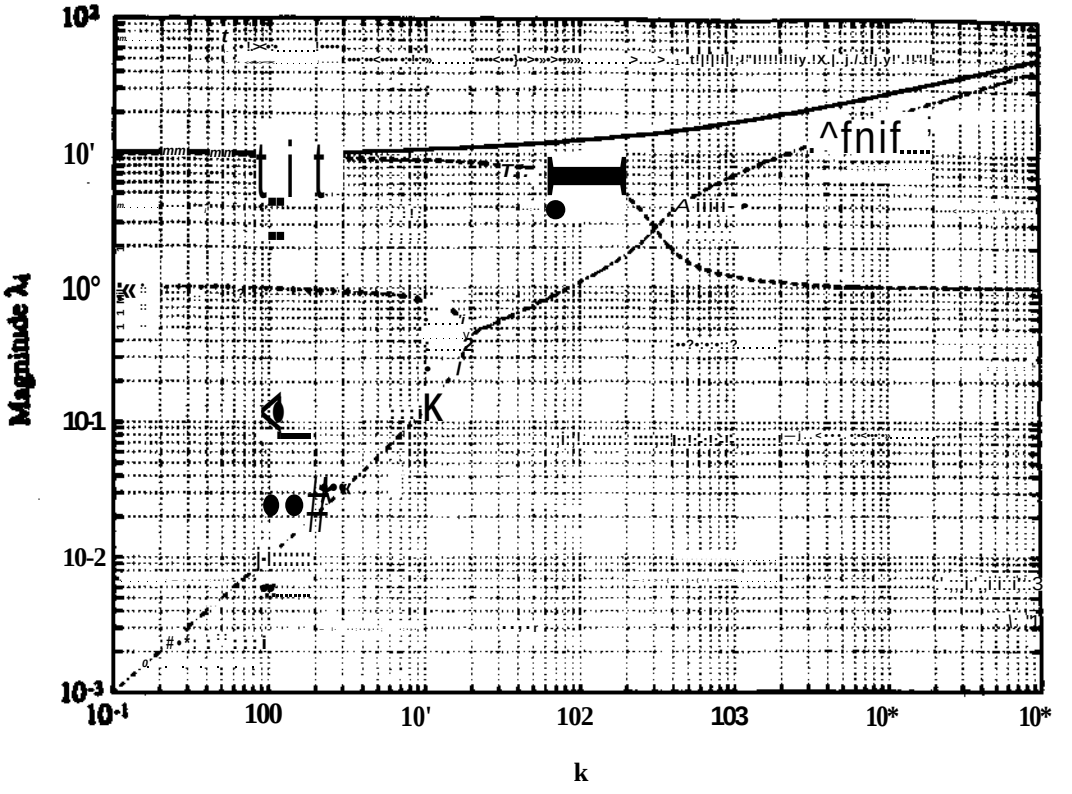

Figure 6a. Magnitude Gain **Plot for Example 2.**

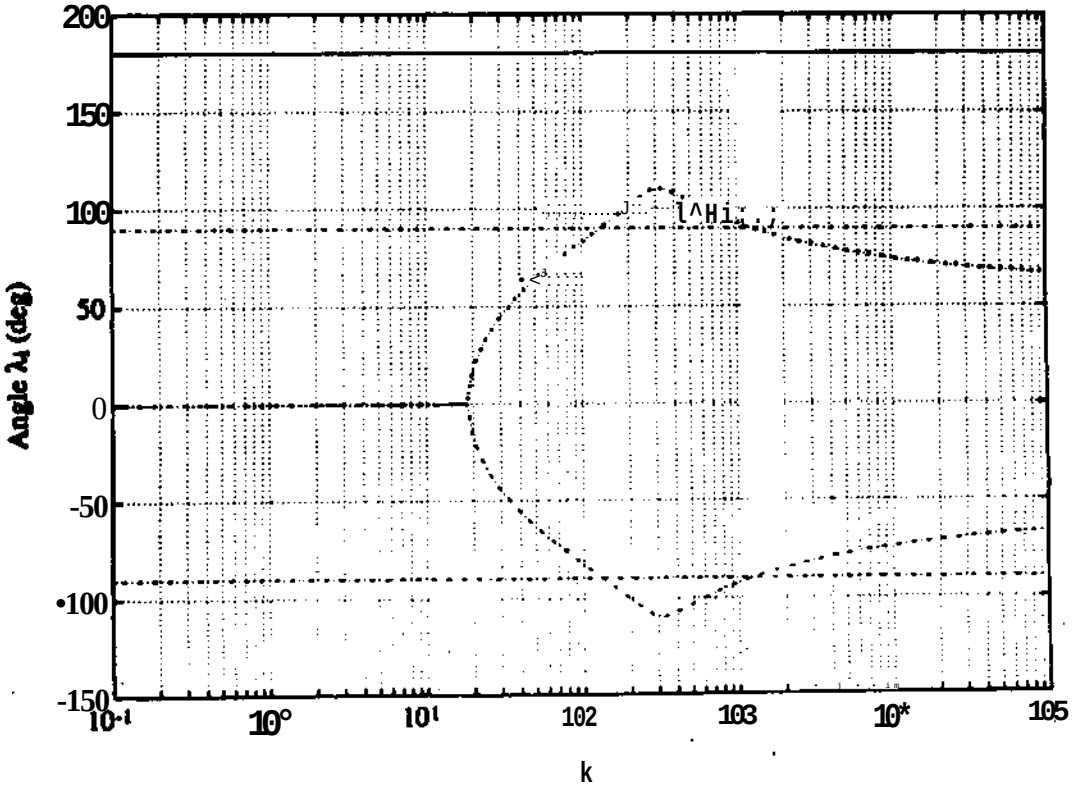

Figure 6b. Angle Gain Plot for Example 2.

Example 3

Here we consider the same system as in Example 2 with a PED controller.

$$g3(s)=\frac{(s+1)^2}{s(s-1)(s+10)^2} \qquad (50)$$

The root locus plot is presented in Figure 7 and shows the two finite eigenvalues approaching the double transmission zero at s = - 1 . As expected from *Theorem 5* **the** approach rate to the double zeros is inversely proportional to $k^{1}\wedge$ since w = 2. This is demonstrated by the high gain slope of -1/2 in Figure 8 which shows the distance to the finite transmission zeros.

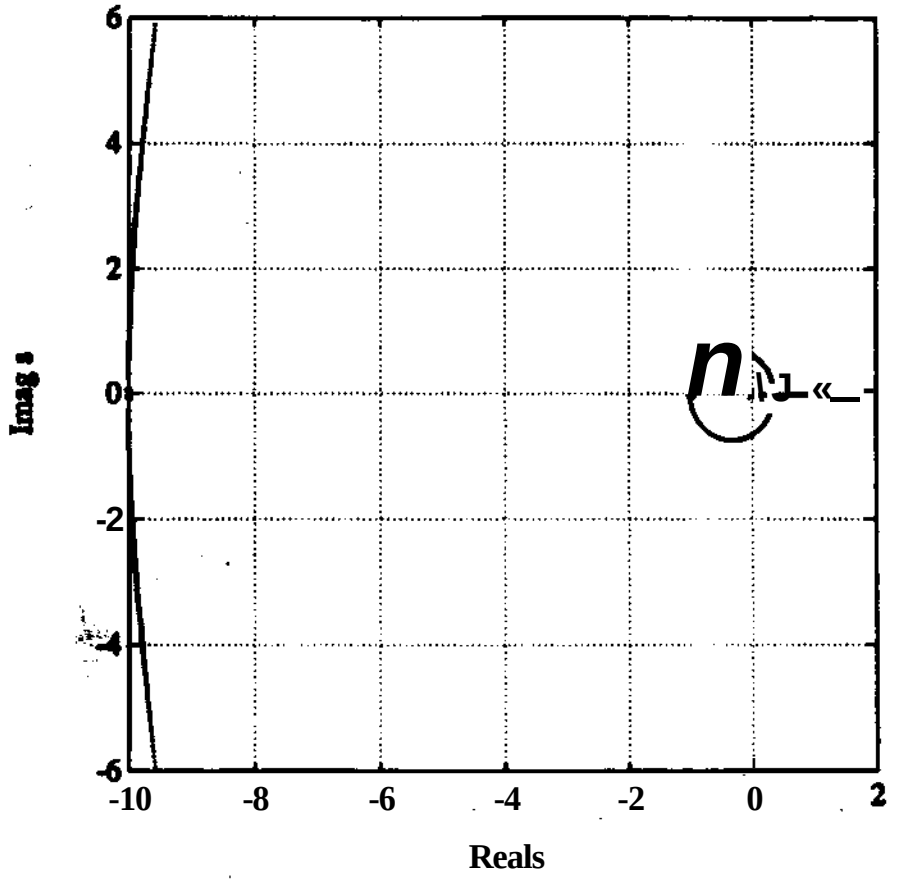

Figure 7. Root Locus Plot for Example 3.

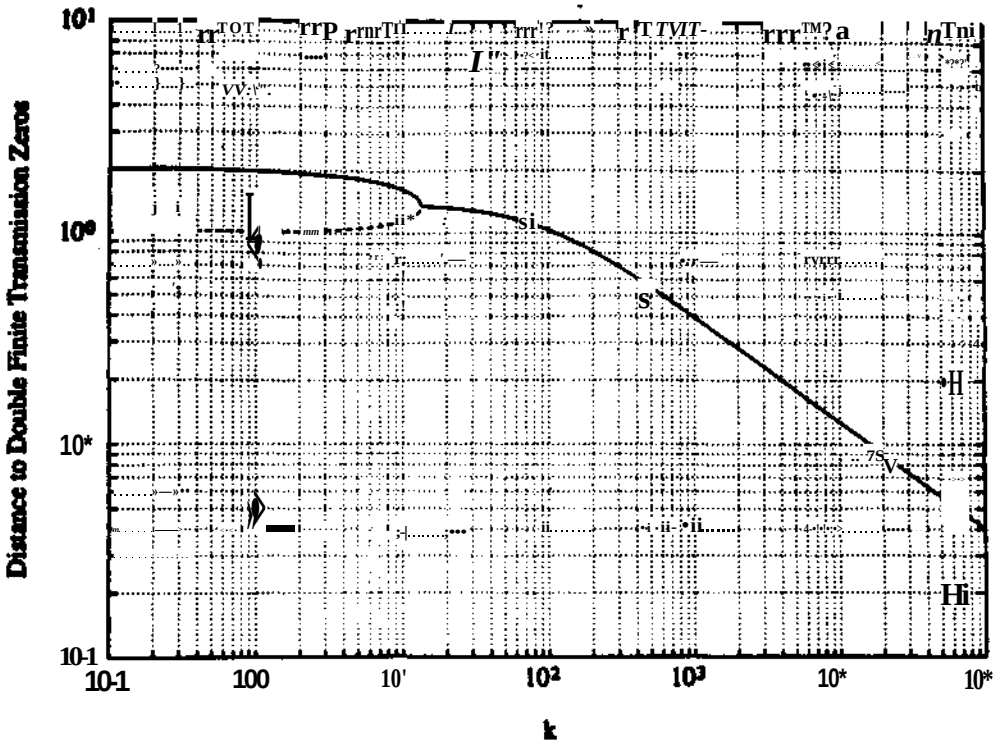

Figure 8. Distance to Double Finite Transmission Zeros for Example 3.

V. Closing

This paper has promoted the use of gain plots that expose closed-loop eigenvalue geometry as a function of a system parameter such as propononal gain. By displaying the eigenvalue magnitude *vs.* gain in a logarithmic plot and the eigenvalue angle *vs.* gain in a semi-logarithmic plot, fundamental concepts of classical control can be determined by inspection. For example, stability, gain margin, root sensitivity, eigenvalue approach rates to both finite and infinite transmission zeros, as well as other properties are available. The gain plots embellish the information presented in the root locus, and are recommended as a powerful new tool for control system analysis and design.

References

[1] Nyquist, H., "Regeneration Theory," BejJSyjitejn Technical Journal, Vol. 11, pp. 126-147, 1932.

[2] Bode, H. W., "Relations Between Attenuation and Phase in Feedback Amplifier resign," Bell System Technical Journal. Vol. 19, 1940, pp. 421^54.

[3] Evans, W. R., "Graphical Analysis of Control Systems," Transactions pj 1kg. American Institute of Electrical Engineers. Vol- 67, 1948, pp. 547-551.